Annals of Nuclear Energy 190 (2023) 109864

Contents lists available at ScienceDirect

Annals of Nuclear Energy

journal homepage: www.elsevier.com/locate/anucene

Hybrid data assimilation methods, Part I: Numerical comparison between GEIM and PBDW

Stefano Riva[1], Carolina Introini[1], Stefano Lorenzi[1], Antonio Cammi [*,1]

Politecnico di Milano, Department of Energy, CeSNEF-Nuclear Engineering Division, Nuclear Reactors Group, -via La Masa, 34, 20156 Milano, Italy

ARTICLE INFO

Keywords:
GEIM
PBDW
Model order reduction
Data assimilation
Thermal hydraulics

ABSTRACT

Hybrid Data Assimilation (HDA) methods are a class of numerical methods that aim at integrating Model Order Reduction (MOR) techniques into a Data Assimilation (DA) framework, thus combining mathematical models and experimental data. The objective is to reduce the solution time using MOR algorithms whilst keeping the accuracy of the models at the desired level using observations, which serve as an update to the a priori prediction of the model. This two-part work investigated HDA techniques by applying them to two classes of problems: numerical benchmark cases (part 1) and experimental facilities (part 2). In particular, this paper discusses the former, focusing on the numerical formulation of the methodologies and on the effect of noisy data. Indeed, real-world experimental data are always polluted by errors and uncertainties; therefore, it is critical to first assess the performance of these techniques on numerical benchmark cases with the artificial introduction of random noise before applying them to real-world experimental facilities. As such, this paper applies the Generalised Empirical Interpolation Method (GEIM) and the Parameterised-Background Data-Weak (PBDW) formulation to a non-adiabatic airflow over the classical computational fluid-dynamics benchmark of the 3D Backward Facing Step (BFS). Results show how both algorithms are valuable tools to reconstruct the state of the system when measurements are available, whilst assessing the effect of noise on the available data; in particular, the GEIM is a bit better than the PBDW since a lower reconstruction error is achieved with fewer sensors.

1. Introduction

The latest achievements in numerical analysis and scientific computing have led numerical simulations in engineering and applied sciences to gain more importance for investigating physical phenomena. Typically, such an analysis relies on solving parameterised Partial Differential Equations (PDEs), commonly referred to as the Full Order Model (FOM) or the *high-fidelity* model. Since a direct analytical solution is rarely available, especially for complex problems, their solution must use standard numerical methods, such as finite elements, finite volumes or spectral methods. Despite the recent developments both regarding computational hardware power and numerical software accuracy, typical engineering problems have a size of $\mathcal{O}(10^6–10^9)$ degrees of freedom, which results in several hours (or even days) of CPU time to numerically solve the system, even on large hardware parallel architectures.

Despite parameterised PDEs being used, for example, for the design and optimisation phase for physical systems (Schilders et al., 2008; Versteeg and Malalasekera, 2007), they are not suited for large systems because of the associated computational cost, especially when quick repetitive solutions are required; in this context, Model Order Reduction (MOR) is a promising tool. In literature, this expression identifies any approach aimed to replace the *high-fidelity* problem with one featuring a much lower complexity (Quarteroni et al., 2015; Hesthaven et al., 2016). This set of techniques, developed originally for control theory, aims to study a dynamical system while preserving its input–output behaviour as much as possible. As the name suggests, MOR tries to reduce the dimension of the model to perform faster simulations while ensuring the preservation of the essential features of the physical phenomena. However, these methods cannot have results as accurate as the FOMs, which can be a critical issue in some applications, for instance, when they require the safe operation of the physical system at all times.

In the last few years, there have also been many improvements in Data Assimilation (DA) (Brunton and Kutz, 2019; Carrassi et al., 2018), which is a mathematical discipline that deals with the combination of theoretical modelling and experimental observations. Nowadays, most

* Corresponding author.
E-mail address: antonio.cammi@polimi.it (A. Cammi).
[1] The authors contributed equally to this work.

https://doi.org/10.1016/j.anucene.2023.109864
Received 9 November 2022; Received in revised form 23 March 2023; Accepted 11 April 2023
Available online 2 May 2023

of these methods use Bayesian techniques or machine learning, which requires training a surrogate model using some *a priori* knowledge. With this approach, the training data from experiments or numerical models feed the surrogate model. For instance, an application of this kind of *meta-modelling* has been used for uncertainty quantification, by means of techniques based on Gaussian processes (Rasmussen and Williams, 2006; Wu et al., 2018a), in thermal-hydraulics systems (Wu et al., 2018b; Wang et al., 2019). Even though this approach can provide accurate predictions, the mathematical background of the model is lost completely. MOR methods, instead, preserve the theoretical structure, for instance, *intrusive* approaches require the knowledge of the governing equations during the Online phase. However, models are usually limited by their accuracy (due to simplifying hypotheses or uncertainties on the parameters), thus, the combination between MOR and experimental data is of interest as the latter can introduce new information not considered by the model whilst the former keeps the mathematical framework.

Of particular interest are Hybrid Data Assimilation (HDA) methods, in which a theoretical prediction, approximated via MOR, is corrected or updated by experimental evaluations of some fields (e.g., the measure of the temperature in a pipe or the neutron flux in a nuclear reactor). This possibility is of interest in several engineering fields, especially in nuclear reactors, which require the control and safety of the system at all times during operation. These are rather complex systems that involve more than one physics (thermal hydraulics, neutronics, thermo-mechanics, chemistry), making a Full Order multi-physics model not feasible for real-time applications; in fact, these high-fidelity models usually are very demanding from the computational point of view, even when using high-performance computers. Furthermore, the HDA approach allows the introduction of evaluations of fields with experimental measurements, which can complete the information of the model itself. The availability of the values of the quantities of interest at critical points of the system is an essential requirement for the safe operation of the system itself. These methods can also perform uncertainty quantification on the parameters characterising the system.

In addition, a critical concern is the correct positioning of experimental sensors to maximise the amount of information extracted by the physical system. MOR methods in a DA framework can address this problem; specifically, this hybrid approach can select a set of points, which typically represent the most critical ones in the system. The correct selection of locations is of great importance for safety, as the experimental measures can provide a direct evaluation at the most critical points (from the point of view of safety).

Among the different classes of MOR methods, reduced basis methods (Quarteroni et al., 2015; Maday and Patera, 2020) are the most widespread. Proper Orthogonal Decomposition (POD) is the state-of-the-art for reduced basis techniques, especially in fluid dynamics (Stabile et al., 2017; Berkooz et al., 1993; Lorenzi et al., 2016) and nuclear applications, due to its superior performance in building reduced spaces. For instance, it has been applied for thermal hydraulics modelling (Vergari et al., 2020), Lead-cooled Fast Reactor analysis (Generation IV International Forum, 2014; Lorenzi et al., 2017) and fuel-burnup calculations (Castagna et al., 2020).

However, the POD-based projection method alone cannot include experimental data; hence, its accuracy is limited by the accuracy of the mathematical model itself, even though some hybrid approaches exist, such as Gappy-POD (Everson and Sirovich, 1995; Willcox, 2006), Fast Field reconstruction (Gong et al., 2021) or a combination with Introini et al. (2018), Kalman (1960), Introini (2021). Other proposed approaches aim at overcoming the limitations of the POD projection (Farhat et al., 2020), such as using techniques able to treat non-affine parametric dependence (Grepl et al., 2007). The Empirical Interpolation Method (EIM) (Maday et al., 2008) is a greedy algorithm introduced for state estimation and sensor positioning in thermal hydraulics systems for both scalar and vector fields (Silva et al., 2021). However, this technique relies on point-wise measurements, which are not always a realistic representation of the data: therefore, the Generalised Empirical Interpolation Method (GEIM) (Maday and Mula, 2013; Maday et al., 2015b, 2016) has been developed to consider a better description of the experimental acquisition. It is a reliable technique already tested on rather complex systems, such as the TRIGA reactor (Fouquet et al., 2003; Introini, 2021).

GEIM belongs to a broader class of HDA methods, for which, in the last years, a more general theory has been developed, resulting in the Parameterised-Backward Data-Weak (PBDW) formulation (Maday et al., 2014; Gong et al., 2019; Maday et al., 2015a; Maday and Taddei, 2019). This theory claims to theoretically describe the mathematical background of HDA methods, aiming at being related to various techniques such as GEIM or Gappy-POD, according to particular choices in the algorithm. This formulation defines a proper representation of the functional spaces of the reduced basis and the experimental update (Section 3).

Every hybrid data assimilation method aims at combining theoretical predictions and experimental observation. Indeed, the mathematical model represents the starting point and the primary source of information (Fig. 1) to generate the reduced space and select the experimental sensors; the experimental data take the role of an update.

In literature, not many works apply GEIM and PBDW to complex system, even few tackles their application to experimental facilities with real-world data (Taddei, 2016; Gong, 2018). Due to the complexity of the real problems, this first part is dedicated to assessing the reliability and the main limitations of GEIM and PBDW when applied to numerical cases, especially considering noisy data: in fact, the former is known to be unstable (Argaud et al., 2017), making necessary the use of stabilisation techniques. In this work, the approach based on the Tikhonov regularisation, proposed in Introini et al. (2023a), is used: the application of this technique to 3D systems is one of the most important outcomes of these work.

Therefore, it is crucial to assess the efficiency of these methods on a numerical case before moving to a real system, to be aware of their main advantages and limitations. In this work, it has been chosen to compare two of the most famous techniques, the GEIM and the PBDW, on the Backward Facing Step with a non-adiabatic flow. As such, the paper is as follows: Sections 2 and 3 present the theoretical background for GEIM and PBDW; then, Section 4 show their results for a relatively simple numerical benchmark case; finally, Section 5 draws the main conclusions along with some hints on future works.

2. Generalised Empirical Interpolation Method (GEIM)

This technique is the natural extension of the EIM, introduced in Grepl et al. (2007) and Maday et al. (2008). Let $\mathcal{U} \subset H^1(\Omega)$ be a Hilbert Space endowed with an inner product and induced norm, usually referred to as the *solution manifold*. In this context, any specific problem can be studied and modelled by a parameterised PDE as

$$\mathcal{G}(u(\mathbf{x}); \mu) = 0 \qquad \mathbf{x} \in \Omega \subset \mathbb{R}^d, \quad d = \{2, 3\}, \tag{1}$$

where $\mathcal{G}$ is a differential operator and μ is a parameter (or a set of parameters)[2] sampled in the domain $D \subseteq \mathbb{R}^p$ ($p \geq 1$). This differential problem will be sometimes referred to as the *best-knowledge* problem, whose solution lies in $\mathcal{U}$.

Assuming the solution of (1) to be a function of a suitable Banach Space with an associated $\|\cdot\|_{L^\infty(\Omega)}$ norm and the Kolmogorov $n-$width[3]

[2] The time t is usually a pseudo-parameter and therefore it is included in μ.

[3] When dealing with MOR methods, a primary role is played by this quantity. It measures to what extent a Banach space can be approximated by a n-dimensional subspace. The notion of Kolmogorov $n-$width allows seeing to what extent the Reduced Basis approximation is good.

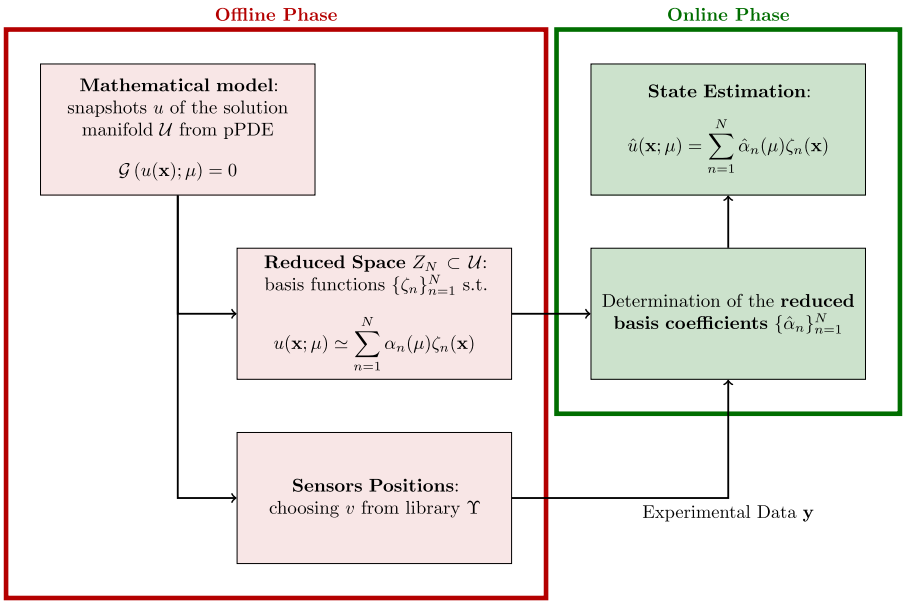

Fig. 1. General idea behind reduced basis methods in a data assimilation framework, used in this paper.

to decrease rapidly with n (Bachmayr and Cohen, 2016; Quarteroni et al., 2015), a proper reduced basis can be created, and accordingly, the solution can be approximated by the interpolant $\mathcal{I}_M$

$$u(\mathbf{x};\mu) \simeq \mathcal{I}_M[u](\mathbf{x}) = \sum_{m=1}^{M} \beta_m(\mu)\cdot q_m(\mathbf{x}), \tag{2}$$

where $\{q_m(\mathbf{x})\}_{m=1}^M$ are called **magic functions**, whereas the reduced basis coefficients $\{\beta_m(\mu)\}_{m=1}^M$ can be found by solving an interpolation problem.

The Generalised Empirical Interpolation Method (GEIM), firstly introduced in Maday and Mula (2013) and further studied in Maday et al. (2015b) and Maday et al. (2016), aims at building hierarchical spaces[4] by using a greedy procedure and by exploiting $Y \subset \mathcal{U}'$, a library of available sensors[5] $v : \mathcal{U} \to \mathbb{R}$, typically dependent on two free parameters: $\mathbf{x}_k \in \Omega$ and $s \in \mathbb{R}^+$, usually referred to as the centre of mass and the point spread, respectively.

GEIM can be reduced to EIM considering a particular kind of sensors, namely $v \equiv \delta$: if the functional is a Dirac's delta, the evaluation of the field is point-wise. At the end of both methods, a subset of points or sensors will be generated: those are called in literature **magic points** or **magic sensors** (respectively for EIM and GEIM) making both algorithms useful for sensor positioning.

2.1. GEIM greedy algorithm

The main ingredients for the GEIM greedy algorithm are the solution manifold $\mathcal{U}$ of functions u, the parameter space $\mathcal{D}$ of μ and the library Y of sensors v. The method exploits an iterative procedure where, at each step M, a reduced space Z_M is generated. As already mentioned, these spaces are hierarchical; this assures that, the more magic sensors and magic functions are considered, the wider the space becomes.

2.1.1. Offline phase

The iterative procedure aims at defining the magic functions and the magic sensors in a greedy manner, by minimising step by step the interpolation error. The complete procedure can be found in Maday et al. (2015b) and it is summarised in Algorithm 1.

Algorithm 1: GEIM continuous version (Offline Stage)

Input
Maximum number of iterations M_{max};
Tolerance tol_{GEIM};
Parametric domain $\mathcal{D}$;

Output
Basis functions $\{q_1(\mathbf{x}),...,q_M(\mathbf{x})\}$;
Linear functionals $\{v_1,...,v_M\}$;

Initialisation
$M=1$, $E_1 = tol_{GEIM}+1$;

First iteration
$u_1 = \underset{u\in\mathcal{U}}{\operatorname{argmax}} ||u||_{L^2(\Omega)}$;
$v_1 = \underset{v\in Y}{\operatorname{argmax}} |v(u_1(\mathbf{x});\mathbf{x}_k,s)|$;
$q_1(\mathbf{x}) = \frac{u_1(\mathbf{x})}{v_1(u(\mathbf{x}))}$;

while $(M < M_{max} \quad \& \quad tol_{GEIM} > E_{M-1})$ **do**
$M = M+1$;
$u_M(\mathbf{x}) = \underset{u\in\mathcal{U}}{\operatorname{argmax}} \left\|u(\mathbf{x};\mu) - \mathcal{I}_{M-1}[u](\mathbf{x};\mu)\right\|_{L^2(\Omega)}$;
given $I_{M-1}[u] = \sum_{m=1}^M \beta_m(\mu)\cdot q_m(\mathbf{x})$;
and $B_{ij}\beta_j = v_i(u)$; $B_{ij} = v_i(q_j)$; $i,j = 1,\dots M$;
$v_M = \underset{v\in Y}{\operatorname{argmax}} \left|v(u_M - \mathcal{I}_{M-1}[u_M];\mathbf{x}_k,s)\right|$;
$q_M(\mathbf{x}) = \frac{u_M(\mathbf{x}) - \mathcal{I}_{M-1}[u_M](\mathbf{x})}{v_M(u_M - \mathcal{I}_{M-1}[u_M])}$;
$E_M = \underset{u\in\mathcal{U}}{\operatorname{argmax}} \left\|u(\mathbf{x};\mu) - \mathcal{I}_M[u](\mathbf{x};\mu)\right\|_{L^2(\Omega)}$;

2.1.2. Online stage

Once the magic functions and the magic sensors have been defined, online monitoring of the system can be performed. The first task consists in collecting the experimental data, i.e. $\{y_m = v_m(u^{true}(\mathbf{x});s)\}_{m=1}^M$, where M represents the maximum number of available sensors, u^{true} is the true field to be reconstructed and $v_m(u(\mathbf{x});s) \equiv v(u(\mathbf{x});\mathbf{x}_m,s)$

[4] The greedy procedure can build larger and larger spaces at each iteration, i.e.

$$X_1 \subset X_2 \subset X_3 \subset \cdots \subset X_{M_{max}} \subset \mathcal{U},$$

given X_k be a Banach space defined at iteration k.

[5] $\mathcal{U}'$ is the dual space of $\mathcal{U}$, where the continuous linear functionals $v : \mathcal{U} \to \mathbb{R}$ on $\mathcal{U}$ live.

represents the evaluation of field $u(\mathbf{x})$ through the functional υ_m. It is important to underline the fact that in real-world applications the data is rarely a perfect measurement since it is usually polluted by random noise. Once the data are collected, the coefficients $\{\beta_m\}_{m=1}^{M}$ can be determined by solving the following linear system of small dimensions

$$B\boldsymbol{\beta} = \mathbf{y} \quad \longleftrightarrow \quad \sum_{m=1}^{M} B_{mn}\beta_m = y_n \qquad n = 1, \dots, M, \tag{3}$$

in which $B_{mn} = \upsilon_n(q_m)$ is the GEIM system matrix. The complete procedure is summarised in Algorithm 2.

For what concerns the computational cost of the online stage, a linear system of size $M \times M$ has to be solved, which requires $\mathcal{O}(M^2)$ operations since the matrix is lower triangular (Maday and Mula, 2013); moreover, the estimation of the state requires $\mathcal{O}(\mathcal{N}_h)$ operations, given $\mathcal{N}_h$ the dimension of the numerical mesh.

Algorithm 2: GEIM continuous version (Online Stage)

Input

Magic functions $\{q_1(\mathbf{x}), ..., q_M(\mathbf{x})\}$;

Magic sensors $\{\upsilon_1, ..., \upsilon_M\}$;

Output

State Estimation $\mathcal{I}_M[u^{true}](\mathbf{x})$;

Acquisition of Experimental Data

$\{y_m = \upsilon_m(u^{true}(\mathbf{x}); s)\}_{m=1}^{M}$;

Online Estimation

Solve the interpolation problem

$B\boldsymbol{\beta} = \mathbf{y}$;

Estimate the state of the system

$u^{true}(\mathbf{x}) \simeq \mathcal{I}_M[u^{true}](\mathbf{x}) = \sum_{m=1}^{M} \beta_m \cdot q_m(\mathbf{x})$

2.2. Well-posedness analysis

Since the matrix B is lower triangular (hence invertible), the GEIM procedure is well-posed, namely, the interpolant exists and it is unique. An estimate for the interpolation error can be derived (Maday et al., 2016) and it can be shown that the error is dependent on the Lebesgue constant Λ_M (Quarteroni et al., 2007) in the $\|\cdot\|_{L^2(\Omega)}$ norm, i.e.

$$\left\|u - \mathcal{I}_{M-1}[u]\right\|_{L^\infty(\Omega)} \leq \left(1 + \Lambda_M\right) \inf_{\psi_M \in Z_M} \left\|u - \psi_M\right\|_{L^\infty(\Omega)}. \tag{4}$$

The Lebesgue constant always enters the interpolation problem and it can be proved to be unbounded (Maday et al., 2008; Quarteroni et al., 2007), indeed this fact represents one of the main drawbacks of interpolation procedures. For this particular case, it can be computed as Maday et al. (2015b). The result in (4) shows that the higher the Lebesgue constant the worst the reconstruction will be and unfortunately Λ_M cannot be bounded and it increases with M. This theoretical result implies that adding a lot of sensors can worsen the GEIM reconstruction, showing that the error is not bounded and that the interpolant does not converge to the true solution with an infinite number of sensors.

2.3. GEIM-stabilisation in presence of random noise

In the previous analysis, the experimental data were considered perfect, meaning that they are not polluted by any kind of disturbance; however, in real-world applications, this is not true. It is common practice to decompose the experimental data as

$$y_m = \upsilon_m(u^{true}) + \varepsilon_m \qquad m = 1, \dots, M \tag{5}$$

where ε_m can represent different kind of disturbances, usually modelled by an uncorrelated zero-mean Gaussian random variable $\varepsilon_m \sim \mathcal{N}(0, \sigma^2)$ with variance σ^2. Under these conditions, it can be seen that the interpolation error bound changes as proved in Argaud et al. (2017)

$$E\left[\max_{\mu \in D} \left\|u - \mathcal{I}_{M-1}[u]\right\|_{L^\infty(\Omega)}\right] \leq \left(1 + \Lambda_M\right) \cdot \left(\inf_{\psi_M \in Z_M} \left\|u - \psi_M\right\|_{L^\infty(\Omega)}\right) + \left(1 + \Lambda_M\right) \cdot \sigma\sqrt{M}, \tag{6}$$

where $E[\cdot]$ is the expected value operator, since the interpolant is now a random variable.

The immediate consequence is that the GEIM is not asymptotically robust in presence of noise, because the error is no more properly bounded and it will increase as more magic functions are added. In the previous section, it has been stated that the Lebesgue constant increases as M increases; moreover, there is a new contribution $\propto \sigma\sqrt{M}$, which makes the error unbounded. Therefore, stabilisation methods are necessary to asymptotically bring the interpolation error down to the noise level σ.

Some stabilisation techniques have been proposed in Argaud et al. (2017), Gong et al. (2022) and Introini et al. (2023a); in this work, the last approach will be used, based on the Tikhonov regularisation (Tikhonov and Arsenin, 1979). The GEIM interpolation problem will be weakened as a least squares minimisation by introducing a penalisation term and later converted into the following linear system:

$$\left(B^T B + \lambda T^T T\right)\boldsymbol{\beta} = B^T \mathbf{y} + \lambda T^T T \langle\boldsymbol{\beta}\rangle, \tag{7}$$

where $\lambda \in \mathbb{R}^+$ is a regularisation parameter to be suitably calibrated,[6] T is the regularisation matrix and $\langle\boldsymbol{\beta}\rangle$ is the sample mean of the coefficients of the train set ($\Xi_{train} \subset \mathcal{D}$), defined as[7]

$$\begin{aligned} T_{ij} &= \sum_{k=1}^{M} \frac{1}{|\sigma_{\beta_k}|}\delta_{ijk} = \begin{cases} \frac{1}{|\sigma_{\beta_i}|} & \text{if } i = j \\ 0 & \text{if } i \neq j \end{cases} && i, j = 1, \dots, M, \\ \sigma_{\beta_i} &= \sqrt{\frac{1}{\dim(\Xi_{train}) - 1} \sum_{\mu \in \Xi_{train}} \left(\beta_i(\mu) - \langle\beta_i\rangle\right)^2} && i = 1, \dots, M, \\ \langle\beta_i\rangle &= \frac{1}{\dim(\Xi_{train})} \sum_{\mu \in \Xi_{train}} \beta_i(\mu) && i = 1, \dots, M, \end{aligned} \tag{8}$$

given δ_{ijk} the Kronecker third-order tensor and σ_β the standard deviation of the coefficients.

Both the system matrix and the right-hand side, Eq. (7), have been modified compared to Eq. (3): in particular, the former is no longer lower triangular, and hence the solution requires $\mathcal{O}(M^3)$ operations. The standard method can be easily retrieved by making the limit for $\lambda \to 0^+$. This version of the GEIM algorithm will be referred to as TR-GEIM.

3. Parameterised-background data-weak (PBDW) formulation

In order to estimate the true state $u^{true} \in \mathcal{U}$ of a system over the domain Ω, two main ingredients are considered: a *best-knowledge* mathematical model, like Eq. (1), and a set of experimental observations $\mathbf{y}^{obs} \in \mathbb{R}^M$, generally decomposed as in Eq. (5). To estimate the true state of the system, the following statement is presented (Carrassi et al., 2018)

$$u_\xi^\star = \underset{u \in \mathcal{U}}{\operatorname{argmin}}\, \xi \left\|u - u^{bk}\right\|_{L^2(\Omega)}^2 + \frac{1}{M}\sum_{m=1}^{M}\left(\upsilon_m(u) - y_m^{obs}\right)^2 \tag{9}$$

where u^{bk} is the solution of the *best-knowledge* model and ξ is called *regularising parameter*, whose job consists in weighting the relative importance of the background (mathematical model) with respect to the experimental data. Such a minimisation problem would require

[6] If the noise level σ is known, the optimal value of λ is σ itself.

[7] There is no unique definition for the matrix T, other options are available (Introini et al., 2023a; Introini, 2021).

solving the mathematical model several times, which is not feasible due to its high computational cost. Therefore, a model order reduction via the reduced basis approach is used, and the $N-$rank approximation $Z_N = span\{\zeta_1, \dots, \zeta_N\}$ of $\mathcal{U}$ is introduced. Then, the state estimation $u_\xi^\star$ is decomposed as $u_\xi^\star = z_\xi^\star + \gamma_\xi^\star$ and accordingly statement (9) can be rewritten as

$$\left(z_\xi^\star, \gamma_\xi^\star\right) = \underset{(z,\gamma)\in Z_N\times\mathcal{U}}{\operatorname{argmin}} \; \xi \|\gamma\|^2_{L^2(\Omega)} + \frac{1}{M}\sum_{m=1}^{M}\left[v_m(z+\gamma) - y_m^{obs}\right]^2 \tag{10}$$

where $z_\xi^\star$ is the approximation of u^{bk} in Z_N.

Eq. (10) is known as the PBDW statement (Maday et al., 2015a; Taddei, 2016; Maday and Taddei, 2019), and the parameter ξ should be calibrated according to the accuracy of the background space and to the magnitude of the disturbance ε_m; this may require the implementation of an adaptive procedure.

The components of the state estimation have a clear interpretation: $z_\xi^\star$ is known as the deduced background, and it represents the information coming from the mathematical model (along with its modelling error), whereas $\gamma_\xi^\star$ is the update that accommodates unanticipated information or non-parametric uncertainty. This formulation is the most general one since it has been designed to consider imperfect measurements. The PBDW was firstly introduced in Maday et al. (2014) for noise-free data

$$\left(z^\star, \gamma^\star\right) = \underset{(z,\gamma)\in Z_N\times\mathcal{U}}{\operatorname{argmin}} \; \|\gamma\|^2_{L^2(\Omega)} \qquad \text{subject to } \left\{v_m(z+\gamma) = y_m^{obs}\right\}_{m=1}^M \tag{11}$$

It can be proved that the two formulations are equivalent when $\xi \to 0^+$, as shown in Taddei (2016). In the following, it will be highlighted that the effect of ξ is an improvement in the convergence properties of the method.

3.1. Well-posedness and a-priori error analysis

Let $R_{\mathcal{U}} : \mathcal{U}' \to \mathcal{U}$ be the Riesz operator from the dual space $\mathcal{U}'$ to the solution space $\mathcal{U}$, defined such that $(R_{\mathcal{U}}v, u) = v(u)$ for any $u \in \mathcal{U}$ and $v \in \mathcal{U}'$; hence, the $M-$dimensional update space $\mathcal{U}_M$ can be characterised as

$$\mathcal{U}_M = span\left\{g_m \triangleq R_{\mathcal{U}}v_m\right\}_{m=1}^M$$

where $\{g_m\}_{m=1}^M$ is a basis for the space itself. Moreover, the following definition is necessary to prove the well-posedness of the PBDW statement:

$$\beta_{N,M} = \inf_{z\in Z_N}\sup_{q\in\mathcal{U}_M}\frac{(z,q)_{L^2(\Omega)}}{\|z\|_{L^2(\Omega)}\cdot\|q\|_{L^2(\Omega)}}, \tag{12}$$

that is, the *inf-sup* constant, which comes with a very important property: it is a non-decreasing function of N and a non-increasing function of M; furthermore, $\beta_{N,M} = 0$ if $N > M$. This fact imposes a constraint on the choice of N and M, specifically the number of sensors M must not be always lower than the dimension of the reduced space N; if this condition is respected, $\beta_{N,M} > 0$ and the PBDW statement (10) admits unique solution (Maday et al., 2014). A complete explanation on the role of the *inf-sup* constant in the estimation error can be found in Maday et al. (2014) and Taddei (2016).

In the end, the structure of the PBDW formulation enables the use of Galerkin error analysis (Quarteroni, 2016) to develop a proper *a priori* error theory (Maday et al., 2014; Taddei, 2016; Maday and Taddei, 2019). Furthermore, it can be proved that $(z_\xi^\star, \gamma_\xi^\star)$ is a solution to the following saddle point problem

$$\begin{cases} \xi(\gamma_\xi^\star, q)_{L^2(\Omega)} + \dfrac{1}{M}\displaystyle\sum_{m=1}^{M}\left[v_m(z_\xi^\star + \gamma_\xi^\star) - y_m^{obs}\right]v_m(q) = 0 & \forall q \in \mathcal{U}_M \\ (\gamma_\xi^\star, p)_{L^2(\Omega)} = 0 & \forall p \in Z_N \end{cases} \tag{13}$$

This result allows the derivation of a rather simple algebraic formulation. Let $A \in \mathbb{R}^{M\times M}$ and $K \in \mathbb{R}^{M\times N}$ matrices, defined as

$$\begin{aligned} A_{mm'} &= \left(g_m, g_{m'}\right)_{L^2(\Omega)} && m, m' = 1, \dots M, \\ K_{mn} &= \left(g_m, \zeta_n\right)_{L^2(\Omega)} = v_m(\zeta_n) && m = 1, \dots M \quad n = 1, \dots, N. \end{aligned} \tag{14}$$

Since the state estimation $u_\xi^\star$ has been decomposed as $\gamma_\xi^\star + z_\xi^\star$ and each term can be expanded onto its basis, i.e.

$$u_\xi^\star(\mathbf{x}) = \sum_{m=1}^{M}\gamma_m \cdot g_m(\mathbf{x}) + \sum_{n=1}^{N} z_n \cdot \zeta_n(\mathbf{x}), \tag{15}$$

and it is the solution of the PBDW statement (10). The coefficient vectors $\boldsymbol{\gamma}_\xi^\star = [\gamma_1, \dots, \gamma_M]^T \in \mathbb{R}^M$ and $\mathbf{z}_\xi^\star = [z_1, \dots, z_N]^T \in \mathbb{R}^N$ are the solution of the following linear system (Taddei, 2016)

$$\begin{bmatrix} \xi M I + A & K \\ K^T & 0 \end{bmatrix} \cdot \begin{bmatrix} \boldsymbol{\gamma}_\xi^\star \\ \mathbf{z}_\xi^\star \end{bmatrix} = \begin{bmatrix} \mathbf{y}^{obs} \\ \mathbf{0} \end{bmatrix} \tag{16}$$

where $I \in \mathbb{R}^{M\times M}$ is the identity matrix. As already mentioned during the previous subsection, the condition that $\beta_{N,M} > 0$ is necessary and it can be guaranteed if $\text{rank}(K) = N$. Moreover, this constant can be computed as the square root of the minimum eigenvalue of the following problem (Taddei, 2016)

$$K^T A^{-1} K \mathbf{z}_n = \lambda_n Z \mathbf{z}_n \qquad n = 1, \dots N \tag{17}$$

where $Z \in \mathbb{R}^{N\times N}$ is defined as $Z_{nn'} = \left(\zeta_n, \zeta_{n'}\right)_{L^2(\Omega)}$.

3.2. Offline–online decomposition

As typically occurs in HDA or MOR methods, the PBDW procedure is divided into an offline (more demanding from a computational point of view) and an online stage (rather fast). The former includes the construction of the reduced space Z_N, the selection of the sensors and the assembly of the matrices, whereas the latter involves the acquisition of the experimental data, the selection of the regularising weight ξ, the solution of the linear system and the state estimation (see Algorithm 3).

In this work, the Weak Greedy Algorithm (Prud'homme et al., 2002) will be used to build the reduced space[8] Z_N, this choice ensures a nearly optimal space in $\|\cdot\|_{L^2}$ comparable to the one generated by POD (Hesthaven et al., 2016). Once this space has been generated, the *update space* has to be defined with a suitable procedure based on some criteria (Maday et al., 2014). In this work, the approximation error is minimised, thus any element outside Z_N is well approximated by the elements of the updated space. This procedure is nothing but the minimisation of the Lebesgue error constant,[9] namely the GEIM greedy algorithm.

For what concerns the computational costs in the online stage, the linear system has dimension $(M + N) \times (M + N)$ with a saddle point structure, which implies that the number of operations required to solve the problem is $\mathcal{O}((M + N)^3)$.

In the end, Table 1 shows a brief comparison between the different methods investigated in this work. In addition to this, it is worth highlight the fact that the PBDW can be seen as the mathematical generalisation of GEIM: indeed, it is defined to accommodate different HDA methods and a more general error theory can be developed (Taddei, 2016; Maday et al., 2014).

[8] The size of the reduced space Z_N is quite important for two main reasons: the best fit error (between the *best-knowledge* solution and the reconstructed one) should be low enough, which implies that N has to be sufficiently "high"; on the other hand, N should be lower than the number of observations M for the sake of the stability of the PBDW formulation.

[9] Maday et al. (2015b) and Gong et al. (2019) stated that minimising the Lebesgue constant is equivalent to maximise the *inf-sup* constant, given $\xi = 0$.

Algorithm 3: PBDW Computational Procedure

Offline Stage

Choose the space $\mathcal{U}$ and a proper norm $\|\cdot\|$;
Generation of Z_N
$\{\zeta_n\}_{n=1}^N$ = WeakGreedy($\mathcal{U}$, N);
Selection of sensors $\{v_m\}_{m=1}^M$;
Compute the matrices of (14);

Online Stage

Acquisition of experimental data $\mathbf{y}^{obs}$;
Solve linear system (16) for $\boldsymbol{\gamma}_\xi^\star$ and $\mathbf{z}_\xi^\star$;
Evaluate the state of the system as
$u_\xi^\star(\mathbf{x}) = \sum_{m=1}^M \gamma_m \cdot g_m(\mathbf{x}) + \sum_{n=1}^N z_n \cdot \zeta_n(\mathbf{x})$;

Table 1
Comparison between the different HDA methods in terms of spectral properties of the matrix, behaviour against random noise and algorithms used to build the reduced and update space.

	GEIM	TR-GEIM	PBDW
Matrix structure	Lower Triangular	Full	Saddle Point
Matrix size	$M \times M$	$M \times M$	$(M+N)\times(M+N)$
Random noise	Unstable	Stable	Stable
Reduced space	Greedy	Greedy	WeakGreedy
Update space	Greedy	Greedy	Greedy

4. Numerical benchmark case: Backward facing step

It is important to compare and assess the reliability of GEIM and PBDW on a numerical case, in which the model is assumed to be perfect, ignoring and considering noisy measurements. This is why, a typical benchmark for CFD codes, with simple geometry, but characterised at the same time by a rather complex flow, has been chosen: the Backward Facing Step (BFS).

4.1. Description of the test case

The benchmark test case will be a 3D model of airflow over a BFS, considering non-adiabatic flow. The geometry is rather simple, nevertheless, the fluid flow shows separation regions and many studies in the literature have addressed this phenomenon (e.g., Armaly et al., 1983; Nadge and Govardhan, 2014; Le et al., 1997).

For the sake of simplicity, a steady state simulation will be performed and the varying parameter will be the inlet velocity; in particular, the following Reynolds number will be used as a reference quantity

$$Re = \frac{\|\mathbf{u}_{in}\|_2 \cdot h}{\nu}, \tag{18}$$

where $h = 49$ mm is the height of the step, ν $[\frac{m^2}{s}]$ is the kinematic viscosity and $\mathbf{u}_{in} = [u_{in}, 0, 0]$ is the inlet velocity. The parameter domain is defined as $Re \in D = [20, 20\,000]$ and the train and test set can be selected as

$$\begin{aligned} \Xi_{train} &= [20 : 100.4 : 20\,000] \qquad \dim(\Xi_{train}) = 200, \\ \Xi_{test} &= [70 : 100.5 : 20\,000] \qquad \dim(\Xi_{test}) = 199. \end{aligned} \tag{19}$$

Different types of flows will be studied, from laminar to turbulent: in fact, as stated in Nadge and Govardhan (2014), for this problem the flow can be considered laminar if $Re \leq 300$ and fully-turbulent if $Re \geq 5000$; in the middle, a transitional flow is established.

Fig. 2 shows the geometry of the system on the xy plane. As already mentioned, the working fluid is air and the governing equations are the Navier–Stokes equations under the Boussinesq approximation and the energy equation (Ferziger and Peric, 2002)

$$\begin{cases} \nabla \cdot \mathbf{u} = 0 & \mathbf{x} \in \Omega \\ (\mathbf{u} \cdot \nabla)\,\mathbf{u} = \nu \Delta \mathbf{u} - \nabla p_{rgh} - \beta \mathbf{g}(T - T_{ref}) & \mathbf{x} \in \Omega \\ \mathbf{u} \cdot \nabla T = \alpha \Delta T & \mathbf{x} \in \Omega \end{cases} \tag{20}$$

where α is the thermal diffusivity, β the thermal expansion coefficient, p_{rgh} a pressure[10] defined as $p - \mathbf{g} \cdot \mathbf{e}_z$ (whose dimensions are pressure over density) and Ω is the domain. The turbulence treatment, when required, will be carried out using a RANS approach, where the velocity is decomposed into an average and a fluctuating field (Davidson, 2015); the problem will be closed using two equations models, in particular, the $k\omega - SST$ is considered.

The boundary $\partial\Omega$ is given by the inlet Γ_{in}, the outlet Γ_{out} and the walls Γ_w, and the boundary conditions are imposed as follows

$$\begin{cases} \mathbf{u} = \mathbf{u}_{in} & \text{on } \Gamma_{in} \\ \dfrac{\partial p}{\partial \mathbf{n}} = 0 & \text{on } \Gamma_{in} \\ T = T_{in} & \text{on } \Gamma_{in} \end{cases} \quad \begin{cases} \mathbf{u} = \mathbf{0} & \text{on } \Gamma_w \\ \dfrac{\partial p}{\partial \mathbf{n}} = 0 & \text{on } \Gamma_w \\ T = T_w & \text{on } \Gamma_w \end{cases} \quad \begin{cases} \dfrac{\partial \mathbf{u}}{\partial \mathbf{n}} = \mathbf{0} & \text{on } \Gamma_{out} \\ p = 0 & \text{on } \Gamma_{out} \\ \dfrac{\partial T}{\partial \mathbf{n}} = 0 & \text{on } \Gamma_{out} \end{cases} \tag{21}$$

where $T_{in} > T_w$; in particular, $T_{in} = 320\,\text{K}$ and $T_w = 300\,\text{K}$. The turbulence quantities have to be defined on the boundary as well: at the outlet, a *zeroGradient* condition is imposed $\left(\frac{\partial}{\partial \mathbf{n}} = 0\right)$, at the wall suitable wall functions are implemented and at the inlet, they are defined as follows

$$\nu_t = \sqrt{\frac{3}{2}} u_{in} \cdot I\, l_t, \qquad k = \frac{3}{2} \cdot (u_{in}\, I)^2, \qquad \omega = \frac{\sqrt{k}}{l_t}, \tag{22}$$

where ν_t is the turbulent viscosity, k the turbulent kinetic energy, ω the turbulence dissipation rate, I is the turbulence intensity[11] and l_t is the turbulence length scale (estimated as $0.07h$).

4.1.1. Numerical discretisation

The governing Eqs. (20) have been solved with the open-source FV solver OpenFOAM (Weller et al., 1998). The mesh contains $\mathcal{N}_h = 375\,000$ cells, with maximum skewness of 0.034 and maximum non-orthogonality of 0.804.

The problem is not time-dependent, hence a steady-state solver is used, namely *buoyantBoussinesqSimpleFoam*. The turbulence treatment is activated if the Reynolds number reaches values higher than 300 (Nadge and Govardhan, 2014; Introini, 2021). The HDA algorithms have been implemented in the OpenFOAM version 6.x environment.

4.2. Offline stage

The GEIM and the PBDW have been applied only to the temperature field[12] $T \in \mathcal{U} \subset L^2(\Omega)$, the library of functionals $Y = \{v(\cdot; \mathbf{x}_k, s)\}_{k=1}^{\mathcal{N}_h}$ is

[10] Its actual dimension are [Pressure/Density], when incompressible fluids are considered the pressure acts as a constraint from a mathematical standpoint.

[11] This quantity is defined as the ratio between the fluctuating part of the velocity and its average and it can be estimated using the following correlation

$$I = 0.16 \cdot Re^{-1/8}$$

provided in ANSYS, Inc. (2016).

[12] The choice of this particular is not limiting, since both GEIM and PBDW can be extended to deal with vector quantities, as $\mathbf{u}$ with a proper definition of the sensors (Silva et al., 2021).

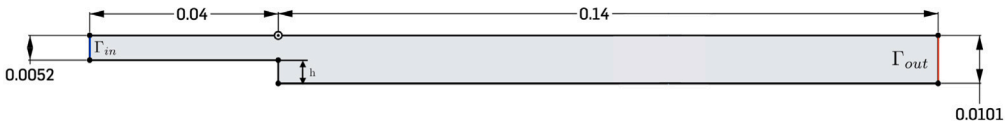

Fig. 2. xy view of the Backward Facing Step (the dimensions are metres).

defined as

$$v_k = v(T(\mathbf{x}); \mathbf{x}_k, s) = \int_\Omega T(\mathbf{x}) \cdot g_k \, d\Omega \qquad \forall T \in \mathcal{U},$$
$$g_k = g(\mathbf{x} - \mathbf{x}_k; s) = \frac{e^{-\frac{\|\mathbf{x}-\mathbf{x}_k\|_2^2}{2s^2}}}{\int_\Omega e^{-\frac{\|\mathbf{x}-\mathbf{x}_k\|_2^2}{2s^2}} \, d\Omega} \qquad \forall \mathbf{x}_k \in \Omega. \tag{23}$$

Different values of the point spread can be used; if $s^2 < 10^6$, the spread is lower than the size of the numerical grid, the GEIM algorithm reduces to EIM (since the functional reduces to a Dirac's distribution) because the measurements become point-wise.

To let the GEIM work at the best of its capability, it is suggested not to introduce any constraints for the sensors selection (Introini et al., 2023b). Nevertheless, if the mesh is too large, the RAM installed on the machine might not be sufficient to save all the sensor functions g_k, because the algorithm generates a function per cell and stores them in the memory. In this case, it has been decided to reduce the required memory by sampling only some cells (still keeping a good coverage of the domain): thus, the reduced domain Ω^* is introduced, so that

$$\Omega^* \subset \Omega \qquad \mathcal{N}_h^* = \dim(\Omega^*) < \dim(\Omega) = \mathcal{N}_h \tag{24}$$

The available locations are thus all $\mathbf{x}_k \in \Omega^*$, given that $\mathcal{N}_h^*$ is much larger than M_{max} (the maximum number of sensors selected). Even though this has been presented as a computational constraint, it mirrors reality: in fact, in real facilities, there are some locations in which sensors cannot be placed.

Error notation. Both in the offline and online stage it is important to see how the selected field is reconstructed via HDA, this is done by using the following definitions. Let $\epsilon(\mathbf{x}; M, \mu)$ be the relative error associated to the field $u^{true}(\mathbf{x}; \mu)$, defined as

$$\epsilon(\mathbf{x}; M, \mu) = \frac{u^{true}(\mathbf{x}; \mu) - \mathcal{P}_M[u^{true}(\cdot; \mu)](\mathbf{x})}{\|u^{true}(\mathbf{x}; \mu)\|_{L^2(\Omega)}}, \tag{25}$$

where $\mathcal{P}_M[u^{true}(\cdot; \mu)](\mathbf{x})$ is an operator which takes as input the true field and returns the reconstructed field using M sensors/basis.[13]

4.2.1. Comparison of the reduced spaces

By focusing on the reduced space, the GEIM and WeakGreedy algorithms will be compared in terms of the relative error defined above. The point-spread s^2 used for the GEIM algorithm will be equal to 10^{-5} for reasons that will be better explained in the next subsection.

Fig. 3 shows the comparison between the two reduced spaces with the one built using POD, which is nearly optimal in L^2-sense (Hesthaven et al., 2016). The WeakGreedy is very close to the POD, and the errors decrease substantially by increasing the dimension of the reduced space Z_N. The GEIM performance is very good as well since a few basis functions can be used to suitably reconstruct the snapshots of the train set: $N \simeq 15$ means a relative error lower than 0.1%. Another remark must be done on the calculation of the coefficients for the linear expansion: indeed, GEIM relies on interpolation, thus it is local algorithm from this point of view, whereas POD and WeakGreedy relies on the projection, which includes the computation of integrals, making them global. This may explain why WeakGreedy seems better when measuring the error in $\|\cdot\|_{L^2(\Omega)}$. Still, both GEIM and WeakGreedy can be used to create reduced spaces.

4.2.2. Analysis of different point-spread values for the sensors

When dealing with the GEIM, it is important to correctly select the point-spread of the functionals: if a real sensor is used, some information can be extracted from the characteristics of the measurement system; however, for this numerical case, its value should be discussed properly, as no *a priori* information.

The analysis of the Lebesgue constant at different values of s, which has a direct impact on the error performed by the method itself, can be used to make a proper decision.

As the value of s increases (Fig. 4), the slope[14] increases as well, in particular for $s^2 = 10^{-3}$ the growth is quite rapid: indeed, the unboundedness of Λ_M is a well-known issue of interpolation problems (Quarteroni et al., 2007). Accordingly, if the point spread value is high, it is not recommended to increase too much the number of magic functions, because the obtained result will be less and less meaningful.

Therefore, s^2 will be taken as 10^{-5}, since at this value the behaviour of the Lebesgue constant is almost steady; furthermore, lower values may be too small and similar to cell size, thus the Gaussian functionals may reduce to Dirac distributions, resulting in the reduction from GEIM to EIM. In real cases, this calibration of value of s^2 is not performed, since the sensitivity of the sensors fixes s^2.

4.2.3. Analysis of the inf-sup stability constant for the PBDW

The *inf-sup* constant plays a very similar role for the PBDW as the Lebesgue constant does for the GEIM. Once the positions of the sensors have been selected with the GEIM greedy algorithm, Eq. (17) can be exploited to find the *inf-sup* stability constant, which involves the calculation of the matrices A and K (Z is the identity matrix, if the basis of the reduced space is orthonormal).

The eigenvalue problem has been solved in MATLAB (The Mathworks, Inc., 2021), which is a more suitable environment when dealing with matrices. The results are displayed in Fig. 5, where different values of N are considered.

In Section 3.1 it has been stated that $\beta_{N,M}$ is a non-decreasing function of M and a non-increasing function of N, the numerical results confirm this statement. Moreover, Fig. 5 highlights the fact that taking a large value of N is not recommended since it would result in a low *inf-sup* constant, providing a less bounded error for the reconstruction. Thus, given a good approximation of the train set, the lower N the better the PBDW performs since the *inf-sup* constant is higher. Finally, the numerical results confirm that, for $M < N$, the *inf-sup* constant is null; this explains why the number of sensors M must always be larger than the number of basis functions N.

[13] For GEIM the number of sensors used and basis number employed is the same, but for PBDW, in the online stage, the dimension of the adopted basis is usually fixed (N) and the varying parameter is the dimension of the updated space $\mathcal{U}_M$.

[14] The y-axis is in logarithmic scale.

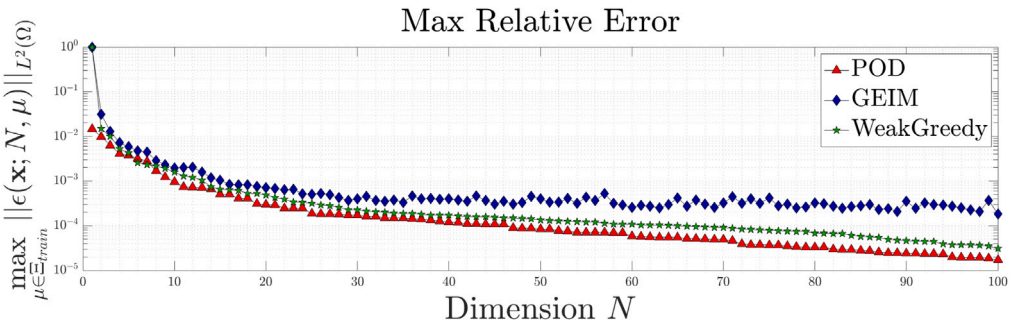

Fig. 3. Maximum relative error measured in $\|\cdot\|_{L^2(\Omega)}$.

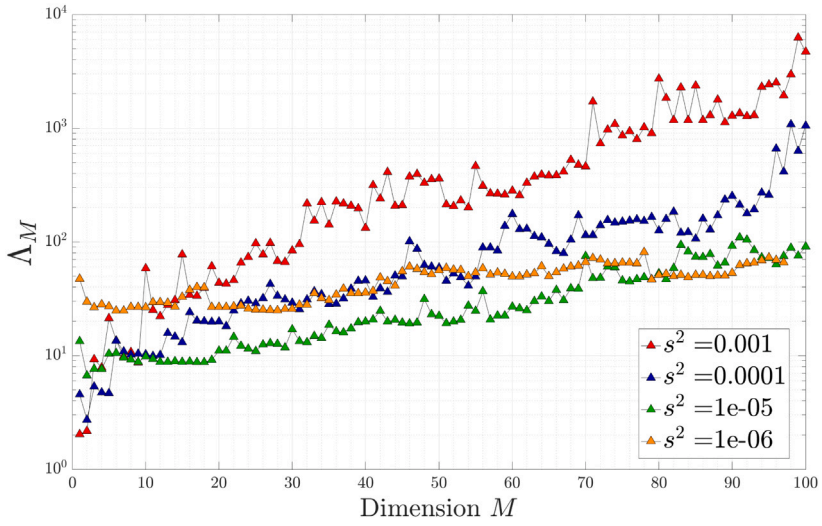

Fig. 4. Lebesgue Constant Λ_M as a function of the number of sensors/magic functions at different point-spread levels.

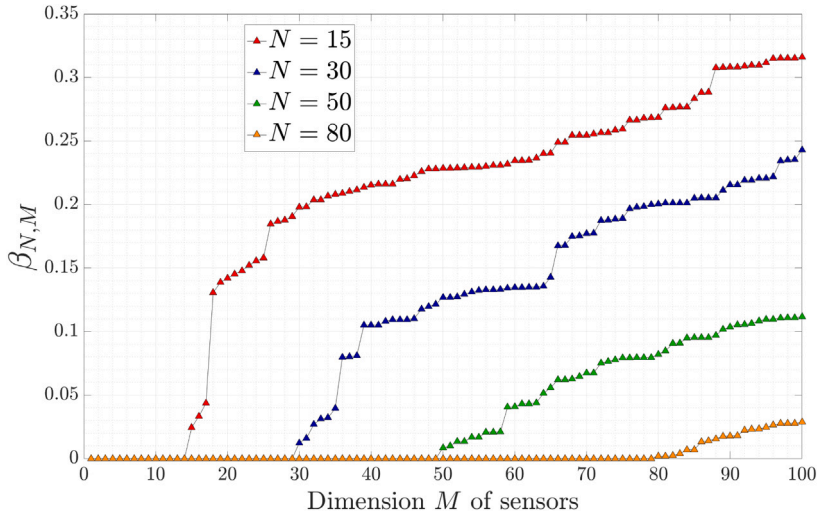

Fig. 5. *Inf-sup* stability constant $\beta_{N,M}$.

4.3. Online stage

These algorithms are suited to integrate models with real experimental data since they claim to be able to reconstruct a certain field (e.g., the temperature) with few sensors along with the information coming from the reduced space. Before diving into this task, it is important to check the performance of the methods against synthetic data, coming from simulations with different parameter values: this is why a test set has been defined in Eq. (19). In the following, the data are assumed to be noise-free or polluted by random disturbance, described from a mathematical standpoint by a zero-mean Gaussian distribution, namely $\varepsilon \sim \mathcal{N}(0, \sigma^2)$.

In the noise-free case, the impact of the dimension of the reduced space N for the PBDW (with $\xi = 0$) will be investigated, then with noisy data a sensitivity analysis on the regularising parameter ξ will be performed to determine its effect.

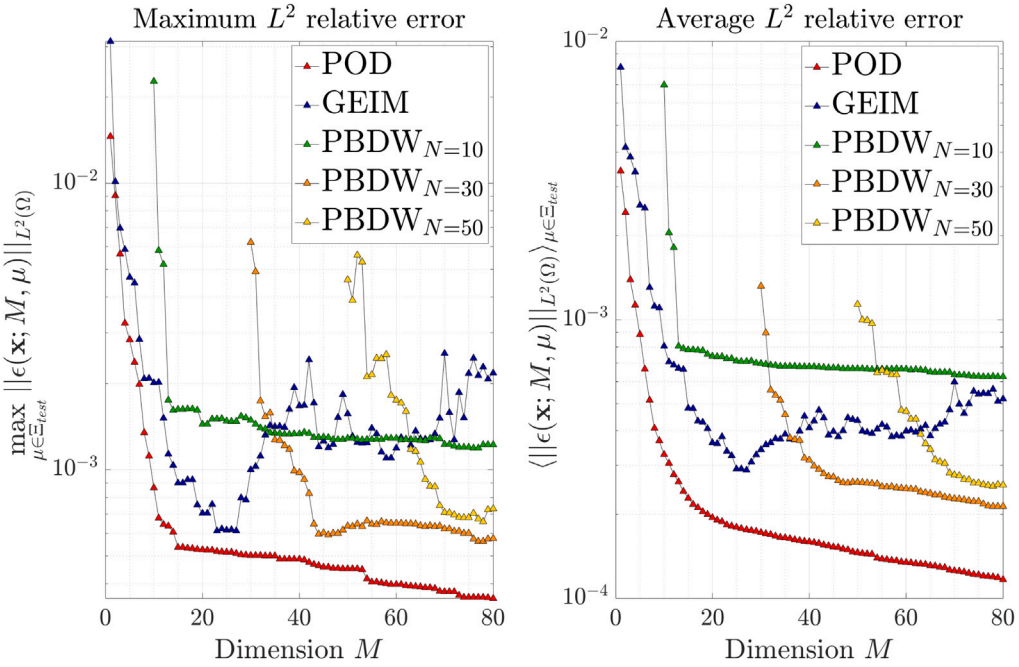

Fig. 6. Maximum and average relative reconstruction error measured in $\|\cdot\|_{L^2(\Omega)}$, for the noise free case.

4.3.1. Synthetic data: noise free

Even though in real applications accessing the true solution is not possible, when synthetic data are used the knowledge coming from the simulations can be further exploited by defining a test set as in Eq. (19). Using the definition of relative error, as in Eq. (25), the maximum and average relative reconstruction error can be analysed.

In Fig. 6, the reconstruction performed by the HDA is plotted and compared with the best possible solution given by the POD.[15] The GEIM algorithm (with point spread $s^2 = 10^{-5}$) produces good estimations, in fact with only 10 magic functions the average relative error is brought below 0.1%, even though it shows some oscillatory behaviour as M increases. For what concerns the PBDW, different dimensions of the reduced space have been considered, in particular $N = [10, 30, 50]$.

The PBDW seems to be more reliable, if the number of sensors is very high, since the error tends better to 0, on the other hand, the GEIM algorithm can bring the error below a certain threshold by employing fewer magic functions/sensors, this is important for real systems in which the number of sensors is typically limited, thus it is necessary to reduce the generalisation error with few sensors.

4.3.2. Synthetic data affected by random noise and impact of the regularising parameter

The behaviour with noisy data is now going to be analysed: at first, the standard algorithms are going to be used, then the Tikhonov regularisation for GEIM and the introduction of the regularising parameter ξ for PBDW are studied. Different values of noises will be investigated, in particular $\sigma = [0.05, 0.1, 0.5, 1]$. For the reduced space in the PBDW formulation, it has been chosen to use $N = 30$ since the reconstruction with noise-free data is very good (Fig. 6).

Fig. 7 shows how random disturbance can affect the average relative reconstruction error; in particular, the unstable behaviour of the GEIM stands out and adding magic functions worsens a lot the estimation. This trend has been theoretically proved in Argaud et al. (2017) and demonstrated in Introini et al. (2023a), Gong (2018) and Gong et al. (2022): the interpolation error increases with the basis number (Eq. (6)). Furthermore, the slope is much affected by the value of random noise, and the turning point for the instability becomes lower as the noise level increases. These effects must be taken into account when dealing with a system with a high level of disturbance.

On the other hand, the PBDW formulation does not suffer from instabilities and a very interesting behaviour occurs, namely, the convergence rate (i.e., the slope) is not a function of the noise level. As depicted in Fig. 7, the black-dashed lines are almost parallel to one another, in particular, they can be represented by a power-law $M^{-\delta}$.

It is then clear that some regularisation must be introduced for the GEIM algorithm to retrieve optimality in the reconstruction. Fig. 8 proves again the reliability of TR-GEIM (Introini et al., 2023a) as a regularisation method: in fact, for the different values of σ, the average relative reconstruction error has been stabilised and adding more magic functions implies a better estimation of the state. Accordingly, this technique has been once again proved to be reliable also on 3D cases, even though an important hypothesis of this analysis is the knowledge of the noise level to calibrate the parameter λ, which may not be trivial when dealing with real-world applications.

Previously, it has been stated that the PBDW formulation is not highly affected by random noise for what concerns instabilities; nevertheless, Fig. 7 shows that the higher the noise level is the higher the average level of the reconstruction error is. In Maday and Taddei (2019), a slightly different formulation has been introduced, which weakens the original PBDW statement (Eq. (11)) with the introduction of the regularising parameter ξ, able to "measure" the importance of the background space compared to the updated one. In the following, the influence of ξ on the reconstruction (i.e., on the error) will be analysed; in this preliminary analysis, a very simple *trial&error* procedure is used to determine the magnitude of this parameter.

Fig. 9 shows the numerical results,[16]: for each noise level, the effect of the parameter ξ is similar, namely the convergence rate changes with ξ. In this case, as the value of the regularising parameter increases, the error tends to better decrease, thus adding more sensors improves

[15] The coefficients of the reduced basis are obtained, through a projection onto the reduced space.

[16] As mentioned in Section 3.1 the value of the parameter ξ may tend to be very large if the model is sufficiently accurate, moreover, if the true solution lies in the reduced space Z_N, it is recommended to pick high values of ξ.

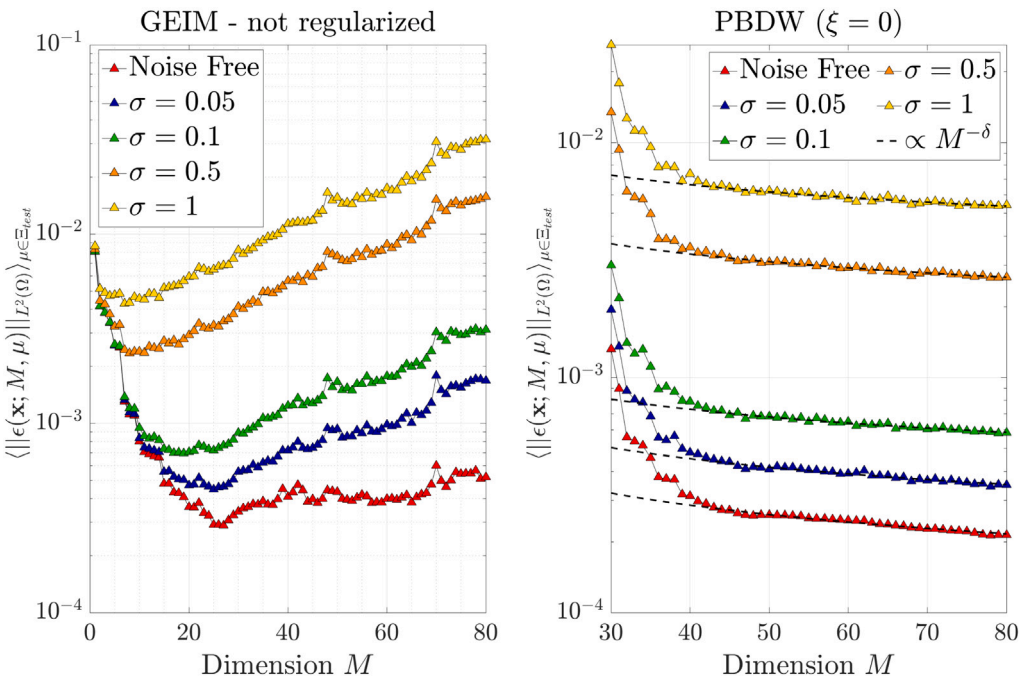

Fig. 7. Average relative reconstruction error with noisy data without regularisation.

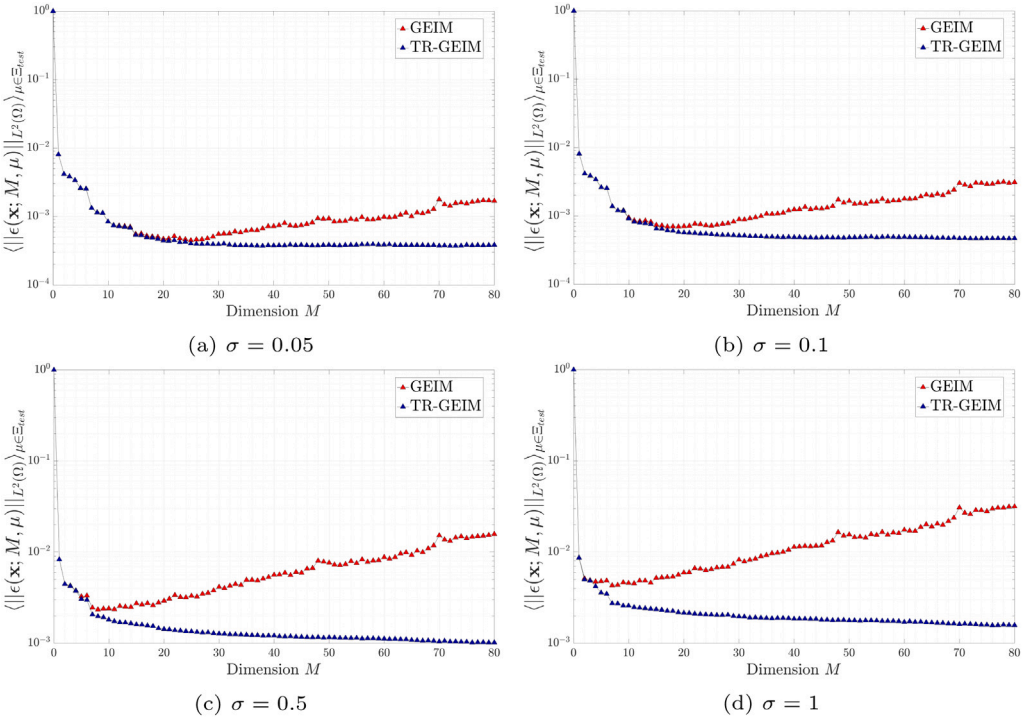

Fig. 8. Average relative reconstruction error using Tikhonov regularisation for the GEIM algorithm at different noise level.

the state estimation. Furthermore, this effect seems to present a sort of "saturation", considering that the case with $\sigma = 0.1$ taking $\xi = 10^5$ or $\xi = 10^6$ produces almost identical results. The improvement in the convergence rate is more evident for large values of the random noise, for instance by taking $\sigma = 0.05$ the effect of the regularising parameter is almost negligible, instead for the case with $\sigma = 1$ the slope changes more.

The numerical results of the different methods have been plotted for the noise level $\sigma = 0.1$.[17] Fig. 10 shows the superiority of TR-GEIM compared to the others, since with 15 magic functions the

[17] This value has been chosen since it is usually encountered in thermal hydraulics systems.

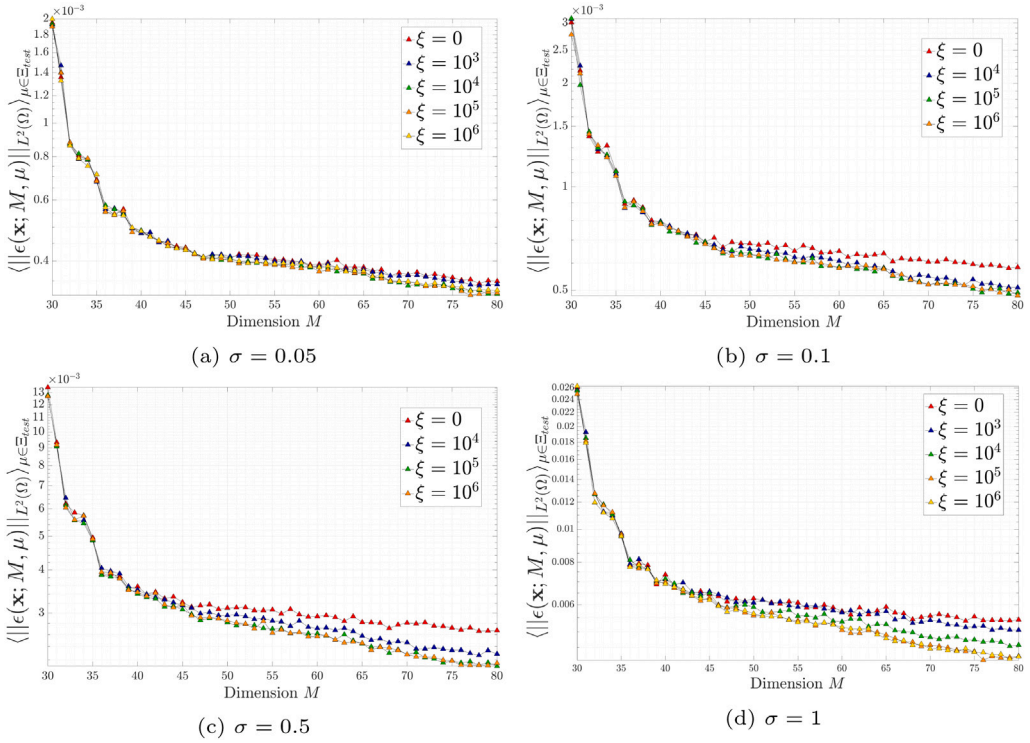

Fig. 9. Average relative reconstruction error using PBDW for different values of ξ at different noise level.

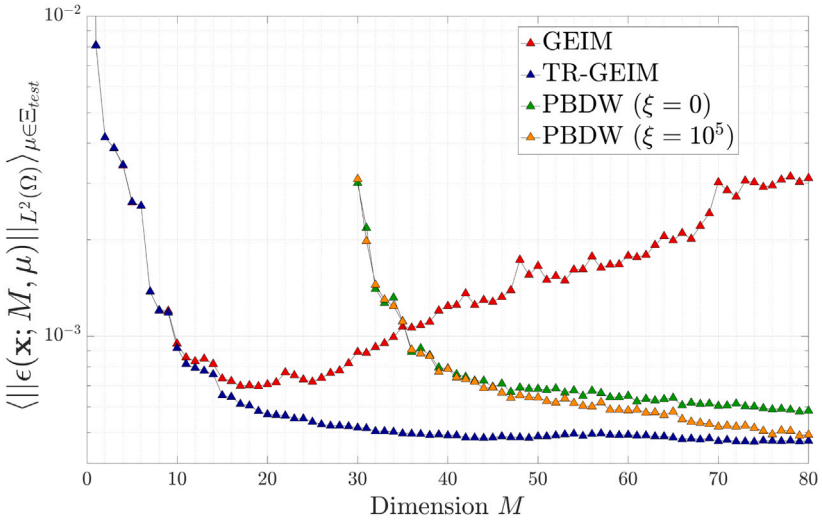

Fig. 10. Comparison of the different HDA methods with noise level $\sigma = 0.1$.

average relative reconstruction error is $\sim 0.06\%$. The PBDW formulation provides the same results by introducing about 40 sensors because there is a lower limit given by N, the dimension of the reduced space. Furthermore, the introduction of the regularising parameter improves the convergence properties: indeed, the slope of the orange markers is less horizontal than the blue ones.

In the end, Fig. 11 shows a contour plot of the true temperature field compared to the reconstructed one, with $Re = 16\,000$. The TR-GEIM shows again its superiority with respect to the others, on the other hand the PBDW seems to suffer a bit near the re-circulation region, this is related to the choice of the WeakGreedy algorithm to build the reduced space.

5. Conclusions

In this work, both the Generalised Empirical Interpolation Method and the Parameterised-Backward Data-Weak formulation have been compared on a numerical case, i.e. the Backward Facing Step, with a non-adiabatic flow, both in the absence and presence of noisy data. These methods are hybrid data assimilation techniques, conceived to combine theoretical modelling and experimental observations, in which Model Order Reduction is coupled with Data Assimilation. They aim at updating the knowledge of the model with the real evaluation of the fields.

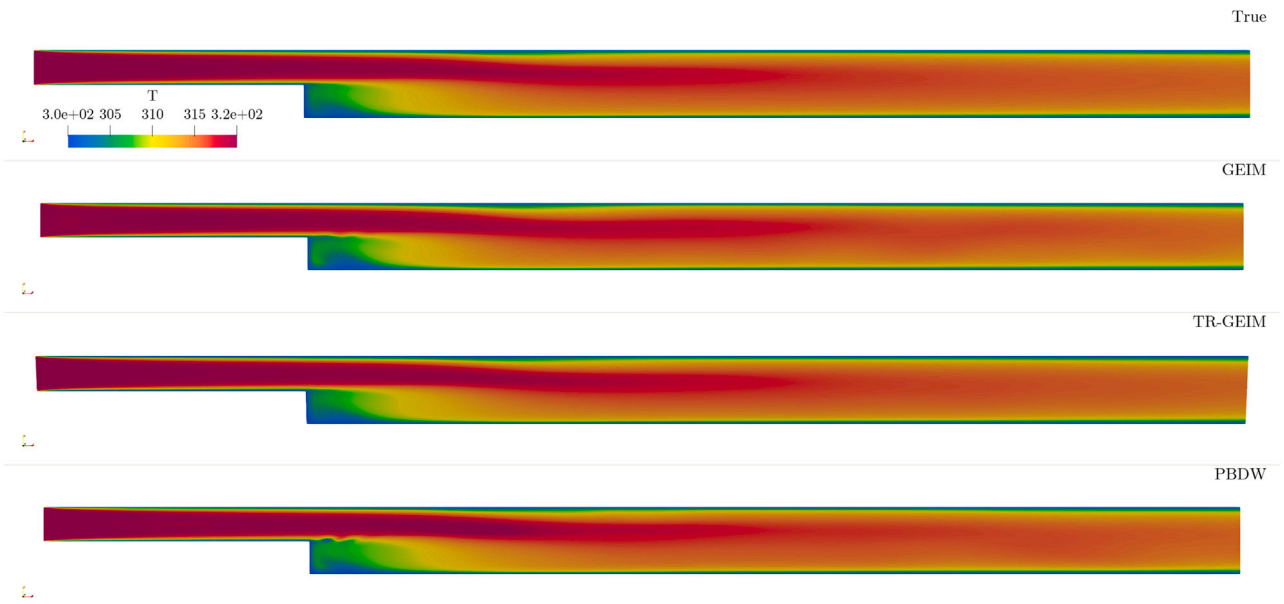

Fig. 11. Contour plots of the temperature field for $Re = 16\,000$, with $M = 60$ and $N = 30$.

For what concerns the efficiency of the techniques, after ensuring the reducibility of the problem, the reconstruction error, in the absence and presence of random noise, can be observed. Considering noise-free data, the GEIM algorithm can reconstruct the field with only 10 magic functions, given an average relative reconstruction error $\sim 0.1\%$, whereas the PBDW formulation has been investigated with 3 different values for the dimension of the reduced space, namely $N = [10, 30, 50]$: all of them can give very good reconstruction; the main downside is the requirement that $M > N$ which may be a problem, because a lot of sensors may be required, which is not always possible to have at disposal, especially for real systems.

Then, random noise has been introduced into the system with 4 different levels $\sigma = [0.05, 0.1, 0.5, 1]$, the standard version of the GEIM presents instabilities: in fact, adding magic functions worsens the reconstruction, therefore the Tikhonov regularisation (TR-GEIM) has been implemented. By considering this new version, the results are very good since the optimality has been retrieved. For what concerns the PBDW, the behaviour is quite different: in fact, this method does not suffer instabilities and the reconstruction error decreases at the same rate for all noise levels considered. In the end, different values of the regularising parameter ξ, whose job consists in weighting the importance of the model compared to the data, have been investigated and its main effect results in improving the convergence rate.

This work can be considered as a benchmark for the performance of these two methods, the GEIM algorithm has once again been proved a very useful tool to be employed in data assimilation problems, especially the TR-GEIM version, on the other hand, the PBDW formulation has shown its superiority in terms of convergence rates and presence of noisy data, nevertheless, it is important to underline that it requires, in general, more sensors to give comparable results with GEIM. Accordingly, the PBDW formulation can be a useful tool, given the reduced space to be small enough.

Finally, the next important step will be to assess the performance of these methods when real experimental data are considered and when a certain model is not perfect, this is the main purpose of the second part. Moreover, an extension of these methods to vector fields and an in-depth comparison of TR-GEIM with the novel regularisation technique by Gong et al. (2022) will be a matter of future development.

List of symbols

Acronyms

BFS Backward Facing Step

CFD Computational Fluid Dynamics

DA Data Assimilation

EIM Empirical Interpolation Method

FOM Full Order Model

GEIM Generalised Empirical Interpolation Method

HDA Hybrid Data Assimilation

LFR Lead-cooled Fast Reactor

MOR Model Order Reduction

PBDW Parameterised-Background Data-Weak

PDE Partial Differential Equation

POD Proper Orthogonal Decomposition

RANS Reynolds Averaged Navier–Stokes

TR-GEIM Tikhonov Regularised-Generalised Empirical Interpolation Method

Greek Symbols

β GEIM coefficients

$\beta_{N,M}$ *Inf-sup* constant with Z_N and $\mathcal{U}_M$ in PBDW

ϵ Relative reconstruction error

ε Random noise

γ Coefficients for the update space in PBDW

λ Eigenvalue, Weight of the Tikhonov regularisation

μ Parameter

σ Standard deviation for random noise

ξ Regularising parameter for PBDW

ζ Reduced basis function in PBDW

Γ Boundary of the physical domain

Λ Lebesgue Constant

Ω Physical domain

Y Sensors library

Ξ Sampled space on $\mathcal{D}$

Latin symbols

g Riesz representation of functional

q Magic Function

s Point spread of the functional

u Generic Snapshot

v Continuous Linear Functional/Experimental sensor

z Coefficients of PBDW for the background space

A Square Matrix of PBDW algebraic problem

B Matrix of GEIM interpolation problem

E Residual field measured in $L^2(\Omega)$

K Rectangular Matrix of PBDW algebraic problem

M Number of sensors/magic functions

N Dimension of the reduced space

Re Reynolds Number

T Tikhonov matrix for the GEIM regularisation, Temperature Field

Z Reduced space

$\mathbf{g}$ Gravity acceleration

$\mathbf{n}$ Normal vector

$\mathbf{u}$ Velocity field

$\mathbf{x}$ Space vector

$\mathbf{y}$ Measurement vector

$\mathcal{D}$ Parameter Space

$\mathcal{G}$ Generic differential operator a PDE

$\mathcal{I}$ GEIM interpolant

$\mathcal{N}$ Gaussian probability distribution

$\mathcal{N}_h$ Size of the numerical mesh

$\mathcal{P}$ MOR operator, whose output is the reconstruction

$\mathcal{U}$ Solution manifold

$\mathcal{U}_M$ Update space in PBDW

Declaration of competing interest

The authors declare that they have no known competing financial interests or personal relationships that could have appeared to influence the work reported in this paper.

Data availability

Data will be made available on request.

References

ANSYS, Inc., 2016. ANSYS fluent - CFD software. URL http://www.ansys.com/products/fluids/ansys-fluent.

Argaud, J.P., Bouriquet, B., Gong, H., Maday, Y., Mula, O., 2017. Stabilization of (G)EIM in presence of measurement noise: Application to nuclear reactor physics. In: Bittencourt, M.L., Dumont, N.A., Hesthaven, J.S. (Eds.), Spectral and High Order Methods for Partial Differential Equations. ICOSAHOM 2016, Springer International Publishing, Cham, pp. 133–145. http://dx.doi.org/10.48550/arXiv.1611.02219.

Armaly, B., Durst, F., Pereira, J., Schönung, B., 1983. Experimental and theoretical investigation of backward-facing step flow. J. Fluid Mech. 127, 473–496. http://dx.doi.org/10.1017/S0022112083002839.

Bachmayr, M., Cohen, A., 2016. Kolmogorov widths and low-rank approximations of parametric elliptic PDEs. Math. Comput. http://dx.doi.org/10.1090/mcom/3132.

Berkooz, G., Holmes, P., Lumley, J.L., 1993. The proper orthogonal decomposition in the analysis of turbulent flows. Annu. Rev. Fluid Mech. 25 (1), 539–575. http://dx.doi.org/10.1146/annurev.fl.25.010193.002543.

Brunton, S.L., Kutz, J.N., 2019. Data-Driven Science and Engineering: Machine Learning, Dynamical Systems, and Control, first ed. Cambridge University Press, USA, URL http://www.databookuw.com.

Carrassi, A., Bocquet, M., Bertino, L., Evensen, G., 2018. Data assimilation in the geosciences: An overview of methods, issues, and perspectives. WIREs Clim. Chang. 9 (5), e535. http://dx.doi.org/10.1002/wcc.535.

Castagna, C., Aufiero, M., Lorenzi, S., Lomonaco, G., Cammi, A., 2020. Development of a reduced order model for fuel burnup analysis. Energies 13 (4), http://dx.doi.org/10.3390/en13040890.

Davidson, P., 2015. Turbulence: An Introduction for Scientists and Engineers. Oxford University Press.

Everson, R., Sirovich, L., 1995. Karhunen–Loève procedure for gappy data. J. Opt. Soc. Amer. A 12 (8), 1657–1664. http://dx.doi.org/10.1364/JOSAA.12.001657.

Farhat, C., Grimberg, S., Manzoni, A., Quarteroni, A., 2020. 5 Computational bottlenecks for PROMs: precomputation and hyperreduction. In: Benner, P., Grivet-Talocia, S., Quarteroni, A., Rozza, G., Schilders, W., Silveira, L.M. (Eds.), Volume 2 Snapshot-Based Methods and Algorithms. De Gruyter, pp. 181–244. http://dx.doi.org/10.1515/9783110671490-005.

Ferziger, J.H., Peric, M., 2002. Computational Methods for Fluid Dynamics, third ed. Springer-Verlag Berlin Heidelberg, p. 426.

Fouquet, D., Razvi, J., Whittemore, W., 2003. TRIGA research reactors: A pathway to the peaceful applications of nuclear energy. Nucl. News 62, 46–56.

Generation IV International Forum, 2014. Technology roadmap update for generation IV nuclear energy systems.

Gong, H., 2018. Data assimilation with reduced basis and noisy measurement : Applications to nuclear reactor cores (Ph.D. thesis). (2018SORUS189), Sorbonne Universitè, URL https://tel.archives-ouvertes.fr/tel-02475840.

Gong, H., Chen, Z., Li, Q., 2022. Generalized empirical interpolation method with H1 regularization: Application to nuclear reactor physics. Front. Energy Res. 9, http://dx.doi.org/10.3389/fenrg.2021.804018.

Gong, H., Chen, Z., Maday, Y., Li, Q., 2021. Optimal and fast field reconstruction with reduced basis and limited observations: Application to reactor core online monitoring. Nucl. Eng. Des. 377, 111113. http://dx.doi.org/10.1016/j.nucengdes.2021.111113.

Gong, H., Maday, Y., Mula, O., Taddei, T., 2019. PBDW method for state estimation: error analysis for noisy data and nonlinear formulation. http://dx.doi.org/10.48550/ARXIV.1906.00810, arXiv arXiv:1906.00810.

Grepl, M.A., Maday, Y., Nguyen, N.C., Patera, A.T., 2007. Efficient reduced-basis treatment of nonaffine and nonlinear partial differential equations. ESAIM: M2AN 41 (3), 575–605. http://dx.doi.org/10.1051/m2an:2007031.

Hesthaven, J., Rozza, G., Stamm, B., 2016. Certified Reduced Basis Methods for Parametrized Partial Differential Equations. Springer International Publishing, http://dx.doi.org/10.1007/978-3-319-22470-1.

Introini, C., 2021. Advanced modelling and stability analysis for nuclear reactors (Ph.D. thesis). Politecnico di Milano.

Introini, C., Cavalleri, S., Lorenzi, S., Riva, S., Cammi, A., 2023a. Stabilization of generalized empirical interpolation method (GEIM) in presence of noise: A novel approach based on Tikhonov regularization. Comput. Methods Appl. Mech. Engrg. 404, 115773. http://dx.doi.org/10.1016/j.cma.2022.115773, URL https://www.sciencedirect.com/science/article/pii/S0045782522007290.

Introini, C., Lorenzi, S., Cammi, A., Baroli, D., 2018. A reduced order Kalman filter for CFD applications. In: Morepas 2018. http://dx.doi.org/10.13140/RG.2.2.31671.01449.

Introini, C., Riva, S., Lorenzi, S., Cavalleri, S., Cammi, A., 2023b. Non-intrusive system state reconstruction from indirect measurements: A novel approach based on Hybrid Data Assimilation methods. Ann. Nucl. Energy 182, 109538. http://dx.doi.org/10.1016/j.anucene.2022.109538, URL https://www.sciencedirect.com/science/article/pii/S0306454922005680.

Kalman, R.E., 1960. A new approach to linear filtering and prediction problems. J. Basic Eng. 82 (1), 35–45. http://dx.doi.org/10.1115/1.3662552.

Le, H., Moin, P., Kim, J., 1997. Direct numerical simulation of turbulent flow over a backward-facing step. J. Fluid Mech. 330, 349–374. http://dx.doi.org/10.1017/S0022112096003941.

Lorenzi, S., Cammi, A., Luzzi, L., Rozza, G., 2016. POD-Galerkin method for finite volume approximation of Navier-Stokes and RANS equations. Comput. Methods Appl. Mech. Engrg. 311, http://dx.doi.org/10.1016/j.cma.2016.08.006.

Lorenzi, S., Cammi, A., Luzzi, L., Rozza, G., 2017. A reduced order model for investigating the dynamics of the Gen-IV LFR coolant pool. Appl. Math. Model. 46, 263–284. http://dx.doi.org/10.1016/j.apm.2017.01.066.

Maday, Y., Anthony, T., Penn, J.D., Yano, M., 2015a. PBDW state estimation: Noisy observations; configuration-adaptive background spaces; physical interpretations. ESAIM: Proc. 50, 144–168. http://dx.doi.org/10.1051/proc/201550008.

Maday, Y., Mula, O., 2013. A Generalized Empirical Interpolation Method: Application of Reduced Basis Techniques to Data Assimilation. In: Springer INdAM Series, Springer Milan, pp. 221–235. http://dx.doi.org/10.1007/978-88-470-2592-9_13.

Maday, Y., Mula, O., Patera, A.T., Yano, M., 2015b. The generalized empirical interpolation method: Stability theory on Hilbert spaces with an application to the Stokes equation. Comput. Methods Appl. Mech. Engrg. 287, 310–334. http://dx.doi.org/10.1016/j.cma.2015.01.018.

Maday, Y., Mula, O., Turinici, G., 2016. Convergence analysis of the generalized empirical interpolation method. SIAM J. Numer. Anal. 54 (3), 1713–1731. http://dx.doi.org/10.1137/140978843.

Maday, Y., Nguyen, N., Patera, A., Pau, G.S.H., 2008. A general multipurpose interpolation procedure: The magic points. Commun. Pure Appl. Anal. 8, http://dx.doi.org/10.3934/cpaa.2009.8.383.

Maday, Y., Patera, A.T., 2020. 4 Reduced basis methods. In: Benner, P., Grivet-Talocia, S., Quarteroni, A., Rozza, G., Schilders, W., Silveira, L.M. (Eds.), Volume 2 Snapshot-Based Methods and Algorithms. De Gruyter, pp. 139–180. http://dx.doi.org/10.1515/9783110671490-004.

Maday, Y., Patera, A., Penn, J., Yano, M., 2014. A parameterized-background data-weak approach to variational data assimilation: formulation, analysis, and application to acoustics. Internat. J. Numer. Methods Engrg. 102, http://dx.doi.org/10.1002/nme.4747.

Maday, Y., Taddei, T., 2019. Adaptive PBDW approach to state estimation: Noisy observations; user-defined update spaces. SIAM J. Sci. Comput. 41 (4), B669–B693. http://dx.doi.org/10.1137/18M116544X.

Nadge, P.M., Govardhan, R.N., 2014. High Reynolds number flow over a backward-facing step: structure of the mean separation bubble. Exp. Fluids 55 (1), 1657. http://dx.doi.org/10.1007/s00348-013-1657-5.

Prud'homme, C., Rovas, D.V., Veroy, K., Patera, A.T., 2002. A mathematical and computational framework for reliable real-time solution of parametrized partial differential equations. Math. Modelling Numer. Anal. 36 (5), 747–771. http://dx.doi.org/10.1051/m2an:2002035.

Quarteroni, A., 2016. Numerical Models for Differential Problems, third ed. Springer, Cham.

Quarteroni, A., Manzoni, A., Negri, F., 2015. Reduced Basis Methods for Partial Differential Equations: An Introduction. In: UNITEXT, Springer International Publishing.

Quarteroni, A., Sacco, R., Saleri, F., 2007. Numerical Mathematics, second ed. Springer, Berlin, Heidelberg, p. 657.

Rasmussen, C.E., Williams, C.K.I., 2006. Gaussian Processes for Machine Learning. MIT Press.

Schilders, W., der Vorst, H., Rommes, J., 2008. Model Order Reduction: Theory, Research Aspects and Applications, Vol. 13. Springer-Verlag Berlin Heidelberg, http://dx.doi.org/10.1007/978-3-540-78841-6.

Silva, F.A.B., Lorenzi, S., Cammi, A., 2021. An empirical interpolation method for two-dimensional vector fields and vector measurements. Internat. J. Numer. Methods Engrg. 122 (15), 3733–3748. http://dx.doi.org/10.1002/nme.6679.

Stabile, G., Hijazi, S., Mola, A., Lorenzi, S., Rozza, G., 2017. POD-Galerkin reduced order methods for CFD using Finite Volume Discretisation: vortex shedding around a circular cylinder. Commun. Appl. Ind. Math. 8 (1), 210–236. http://dx.doi.org/10.1515/caim-2017-0011.

Taddei, T., 2016. Model order reduction methods for data assimilation; state estimation and structural health monitoring (Ph.D. thesis). Massachusetts Institute of Technology, http://dx.doi.org/10.13140/RG.2.2.16001.45928.

The Mathworks, Inc., 2021. version 9.10.0.1739362 (R2021a) Update 5. The Mathworks, Inc., Natick, Massachusetts.

Tikhonov, A.N., Arsenin, V.Y., 1979. Solutions of Ill-Posed Problems. 21, pp. 266–267. http://dx.doi.org/10.1137/1021044,

Vergari, L., Cammi, A., Lorenzi, S., 2020. Reduced order modeling approach for parametrized thermal-hydraulics problems: inclusion of the energy equation in the POD-FV-ROM method. Prog. Nucl. Energy 118, 103071. http://dx.doi.org/10.1016/j.pnucene.2019.103071.

Versteeg, H.K., Malalasekera, W., 2007. An Introduction to Computational Fluid Dynamics: The Finite Volume Method. Pearson Education Limited.

Wang, C., Wu, X., Kozlowski, T., 2019. Gaussian process–based inverse uncertainty quantification for TRACE physical model parameters using steady-state PSBT benchmark. Nucl. Sci. Eng. 193 (1–2), 100–114. http://dx.doi.org/10.1080/00295639.2018.1499279.

Weller, H.G., Tabor, G., Jasak, H., Fureby, C., 1998. A tensorial approach to computational continuum mechanics using object-oriented techniques. Comput. Phys. 12 (6), 620–631. http://dx.doi.org/10.1063/1.168744.

Willcox, K., 2006. Unsteady flow sensing and estimation via the gappy proper orthogonal decomposition. Comput. & Fluids 35 (2), 208–226. http://dx.doi.org/10.1016/j.compfluid.2004.11.006.

Wu, X., Kozlowski, T., Meidani, H., Shirvan, K., 2018a. Inverse uncertainty quantification using the modular Bayesian approach based on Gaussian process, part 1: Theory. Nucl. Eng. Des. 335, 339–355. http://dx.doi.org/10.1016/j.nucengdes.2018.06.004, URL https://www.sciencedirect.com/science/article/pii/S0029549318306423.

Wu, X., Kozlowski, T., Meidani, H., Shirvan, K., 2018b. Inverse uncertainty quantification using the modular Bayesian approach based on Gaussian process, part 2: Application to TRACE. Nucl. Eng. Des. 335, 417–431. http://dx.doi.org/10.1016/j.nucengdes.2018.06.003, URL https://www.sciencedirect.com/science/article/pii/S0029549318306411.